

# Variations in Morphological and Electrical Properties of Pb-doped CdS Thin Films Synthesized in Chemical Baths of Different Acidity

A.I. Onyia

**Abstract:** Using chemical bath deposition technique, lead-doped cadmium sulphide thin films of different grades were synthesized in chemical baths of different pH in polyvinyl polymer matrix and the effects of controlled acidity of growth medium studied with emphasis on film morphology and resistivity. X-ray diffraction was used to obtain film structure while four point probe technique was applied to obtain film electrical resistivity to be between 64  $\Omega\text{m}$  and 105  $\Omega\text{m}$ . Good grades of Pb-doped CdS semiconductor were enabled within the polymer capping and the surface morphology revealed good film which orderliness improved with pH increase. Rutherford backscattering done on the film showed that pH values of growth bath determined elements percentage abundances with impurity level varying from 2.15 % to 2.19 %.

**Index Terms**— CdS, chemical bath deposition, percentage abundance, polymer matrix.

## 1 INTRODUCTION

Cadmium sulphide thin film has, for quite some time, been an important semiconductor to be researched on. It has wide range of applications in various piezo-electronic, optoelectronic, and semi conducting devices [1,2]. CdS has wide band gap of 2.45 eV [3] which is at the middle of electromagnetic spectrum and therefore are of considerable interest for their efficient use in the fabrication of solar cells [4]. Because of its optical properties, CdS is used in CdTe devices as an optical window [5]. In thin film (TF) form, its band gap and other film properties can be altered depending on factors that may include film thickness, grain size, crystal phase, types and levels of impurities *et cetera*. These factors are influenced by the techniques employed in the thin film fabrications. Such techniques include physical vapour deposition (PVD), chemical vapour deposition (CVD), electrochemical deposition (ECD), and chemical bath deposition (CBD) [6-8].

In this work the technique used was CBD which is a low temperature technique that is easily reproducible. It is also adapted for large and irregular surface coverage of nanofilms. However, CdS thin film has poor conductivity and as low as  $10^{-8} \Omega^{-1}\text{m}^{-1}$  has been reported [9]. In order to overcome this problem, doping and post deposition heat treatments are used [10-12]. In this work, Pb-doped CdS were grown in baths that had different bath pH to check the effect of acidity on morphology and electrical properties. These will enable good optimization of the semiconductor for specific applications. The semiconductor synthesis was in polymer capping to ensure early formation of monomers that easily grew into

continuous crystallites. Such crystallites, for this case of polyvinyl alcohol, became small grained that is known to increase crystal semiconductivity [13]

## 2 MATERIALS AND METHODS

The preparation of CdS thin film with the lead impurity was with a chemical 50 ml beaker onto which was mixed 5.1 ml of 0.7 M  $\text{CdCl}_2$ , 3.3 ml  $\text{NH}_3$  (aqu.) solution, 4.0 ml of 0.8 M thiourea ( $\text{NH}_2\text{CSNH}_2$ ) and 35 ml of polyvinyl alcohol (PVA) while stirring for 35 s. Lead doping was accomplished by adding onto the solution 3.5 ml of 0.1M  $\text{Pb}(\text{NO}_3)_2$  while still stirring vigorously. Care was taken not to add excess quantity of lead nitrate that could introduce greater Pb atoms more than 3 % of the abundance of Cd atoms in order to ensure preservation of existing hexagonal phase of cadmium sulphide [14] while increasing film electrical conductivity. Ammonia was used to alter the pH of bath and to complex the reaction in order to have a controlled precipitation that was basically due to the hydrolysis of thiourea in alkaline solution containing cadmium and lead salts. The PVA solution was prepared by adding 450 ml of distilled water to 0.9g of solid PVA ( $\text{C}_2\text{H}_4\text{O}$ )<sub>n</sub> (where n = 1700), and stirring by a magnetic stirrer at 90 °C for 1 h. The solution was aged down to room temperature (288 K) [15]. The PVA presented a matrix for orderly capping and formation of more orderly but smaller CdS crystallites. [16]. A substrate of plane glass slide that was previously degreased in concentrated hydrochloric acid, washed in detergent solutions, rinsed with distilled water and drip dried in dust free environment was vertically inserted

Author: Dr. A.I. Onyia, Enugu State University of Science and Technology, Enugu, Nigeria. E-mail: [ikeaonyia@yahoo.com](mailto:ikeaonyia@yahoo.com)

into the solution and suspended from a synthetic foam that rested on top of the beaker. The acidity of the bath was taken with a pH digital meter to be 9.0. The bath was left for 2 h at room temperature. When the solution ionic product exceeded the solubility product, controlled precipitation of grayish lead-doped CdS occurred on the surface of the glass substrate which was removed, rinsed in distilled water and left to drip dry in dust free air and labeled 15A. Aqueous ammonia, a base with a pH of 11.5, was used to increase the pH of the bath. When in water, however,  $\text{NH}_3$  can dissociate into  $\text{NH}_4^+$  and  $\text{OH}^-$  and hence decrease the pH. The exact pH value of chemical baths used was taken with a digital pH meter. The freshly grown film was annealed for an hour at 150 °C to further increase the crystallite sizes as well as the film electrical conductivity [17].

The experiment was repeated three other times except that the quantities of ammonia used were altered as shown in table 1 which resulted in bath pH as also shown in the same table. Thus in all, four different deposit samples 15A, 15B, 15C and 15D were obtained.

Table 1: Bath pH when ammonia was added

| Vol. of $\text{NH}_3$ (ml) | pH of bath | Sample |
|----------------------------|------------|--------|
| 3.3                        | 9.0        | 15A    |
| 5.0                        | 9.2        | 15B    |
| 7.2                        | 9.6        | 15C    |
| 9.0                        | 10.3       | 15D    |

The structure of thin films deposits was deciphered with Philips X'Pert PRO diffractometer which used a radiator of wavelength  $\lambda = 0.15406 \text{ nm}$  ( $\text{CuK}_\alpha$ ) to scan sample thin films continuously from  $2\theta = 10^\circ$  to  $99^\circ$  in step size of  $0.017^\circ$  at a room temperature of 288 K.

QUADPRD Model 301 auto calculating four point probe was used to profile film surface for electrical resistivity and sheet resistivity of the freshly grown semiconducting thin films. The technique required separate pairs of current-carrying and voltage-carrying electrodes to make accurate measurement of resistivity. When the probes simultaneously contacted the thin semiconductor and the probe separations were same =  $s$ , the resistivity could be given [18] as:

$$\rho_m = 2\pi s \frac{V}{I} \quad 1$$

where the subscript m indicated a case of measured resistivity when the potential difference and current are  $V$  and  $I$ . The measured value,  $\rho_m$  is equal to the actual value  $\rho$  only if the semiconductor sample is of infinite size. For finite thin film, therefore, there will be a correction factor. If the distance from any probe to the nearest boundary is, at least  $5s$ , no correction is needed. Similarly, no correction is required for  $t/s > 5$  where  $t$  is the thickness of sample. When  $t < 5s$ , the thickness correction factor,  $a$  is included as follows:

$$\rho = a 2\pi s \frac{V}{I} \quad 2$$

Thin films fabricated in this exercise had very small thickness of order of nanometres, hence  $\ll s$  and current ringed out from probe points, instead of spheres as in bulk three dimensional crystals. The differential resistance is given as:

$$\Delta R = \rho \frac{dx}{dA} \quad 3$$

Hence,

$$R = \int_{x1}^{x2} \rho \frac{dx}{2\pi x t} \quad 4$$

where  $2\pi x t$  is the cross-section area of thin film of thickness  $t$  [18]. Therefore,

$$\begin{aligned} R &= \int_{x1}^{x2} \rho \frac{dx}{2\pi x t} \\ &= \int_s^{2s} \rho \frac{dx}{2\pi x t} = \frac{\rho}{2\pi x t} \ln 2 \end{aligned} \quad 5$$

Therefore,

$$\begin{aligned} \rho &= 2\pi R t / \ln 2 \\ &= \frac{2\pi t}{\ln 2} \left( \frac{V}{I} \right) \end{aligned} \quad 6$$

We can generally express the sheet resistivity as  $\rho/t = R_s$ , where:

$$R_s = k \left( \frac{V}{I} \right) \quad 7$$

and  $k$  is a geometric factor which does not depend on the probe spacing. In fact [18]:

$$k = \frac{2\pi}{\ln 2} = 9.0 \quad 8$$

### 3. RESULTS AND DISCUSSIONS

#### 3.1 Surface Morphology Study

The morphology of the surface of the thin films grown at different bath pH was as shown in Figs. 1a, 1b, 1c and 1d respectively. Fig. 1a shows that the deposited film has low pothole density which was likely to be the presence of some voids and crystal site vacancies. It however indicated a good crystalline quality and the film surface had generally smooth and dense morphology. Fig. 1b, 1c and 1d micrographs revealed that the deposits concerned had less of these defects as pH of bath increased. All figures revealed that films were polycrystalline in nature.

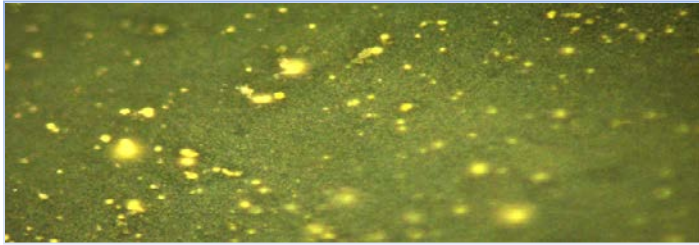


Fig. 1a: Micrograph of Pb-doped CdS thin film (1000X) at bath pH of 9.0

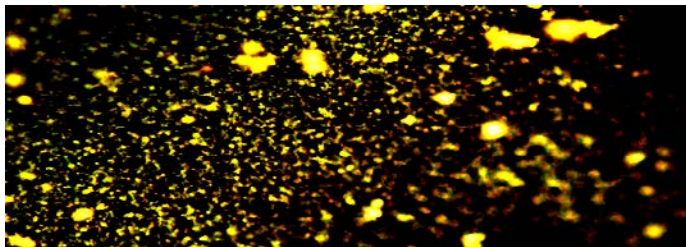


fig. 1b: Micrograph of Pb-doped CdS thin film (1000X) at bath pH of 9.2

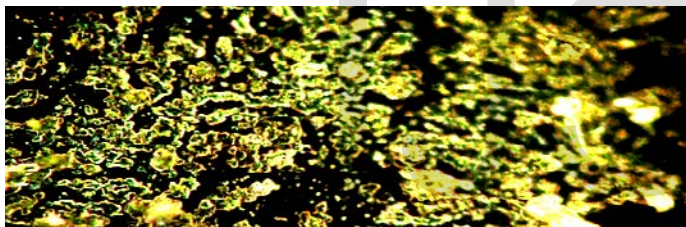


Fig. 1c: Micrograph of Pb-doped CdS thin film (1000X) at bath pH of 9.6

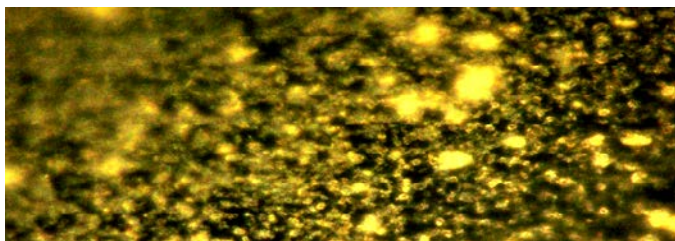


Fig. 1d: Micrograph of Pb-doped CdS thin film (1000X) at bath pH of 10.3

### 3.2 XRD Results

The X-ray diffraction pattern obtained for thin film grown at bath pH of 9.0 (sample 15A) is as shown in Fig. 2 which revealed very ordered film structure with prominent peaks and patterns that identified the film as hexagonal cadmium lead sulphide crystals. Low grade doping as done in this exercise thus, as expected, did not alter the crystalline hexagonal structure of CdS. From the full width at half maximum of X-ray intensity (FWHM) ie  $\beta$ , Debye Scherrer's relation [19, 20]:

$$D = \frac{0.89\lambda}{\beta \cos \theta} \quad 9$$

was used to calculate the average size, D of crystal grain where the X-ray wavelength used was  $\lambda$  and the angle of diffraction was  $\theta$ . Such calculated grain size was as shown in table 2 for film of bath pH = 9.0. Similar calculations for films of varying bath pH revealed that the grain size of the thin films increased with bath pH.

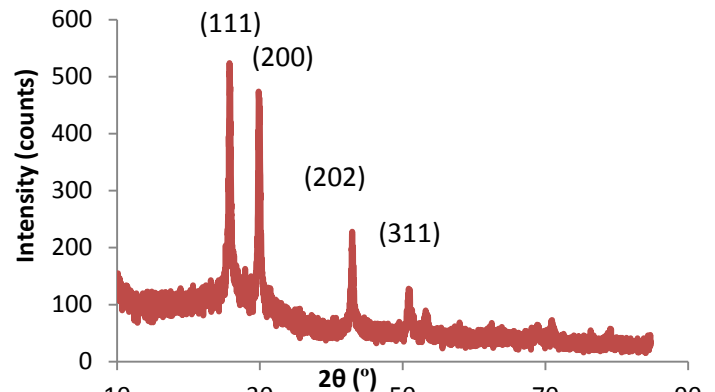


Fig. 2: XRD pattern of Pb-doped CdS TF

Table 2: XRD result for Pb-doped CdS, Card No. 03-065-61623

| (h k l) | d(A°)  | 2θ (°) | FWHM   | D(nm) |
|---------|--------|--------|--------|-------|
| (1 1 1) | 6.4743 | 26.05  | 0.7483 | 20.61 |
| (2 0 0) | 6.0743 | 30.15  | 0.7084 | 22.64 |
| (2 0 2) | 5.1344 | 43.07  | 0.7930 | 23.28 |
| (3 1 1) | 4.9874 | 50.01  | 0.6508 | 21.34 |

Average D: 21.97m

### 3.3 Compositional Results.

The result of Rutherford backscattering elemental analysis was as shown in Fig. 3 for sample thin film grown in bath of pH 9.0. The elements in the substrate (layer 2) and in the deposit (layer 1) confirm that the synthesized thin film actually comprised only Cd, S and small quantity of lead atoms (2.19 %). This small quantity justifies why Pb became only impurity (dopant) to the useful cadmium sulphide thin film semiconductor but did not disorganize its crystal arrangement. Such doping typically improved the conductivity of CdS [21, 22]. Note that the thickness and composition of glass substrate were unaffected in the growth processes. Similar RBS analysis were done for films grown in different bath pH (micrographs not shown) and the effects on film composition were as shown in table 3. It could easily be seen that as pH increased, the percentage of Pb decreased while that of S increased.



Table 3. Percentage abundance of elements in Pb-doped CdS as bath pH changed

| Sample | pH of bath | Percentage Cd | Percentage Pb | Percentage S |
|--------|------------|---------------|---------------|--------------|
| 15A    | 9.0        | 54.27         | 2.19          | 43.54        |
| 15B    | 9.2        | 53.35         | 2.18          | 44.47        |
| 15C    | 9.6        | 53.30         | 2.15          | 44.55        |
| 15D    | 10.3       | 51.01         | 2.15          | 46.84        |

Table 4. Resistivity and sheet resistance of films grown in chemical baths of different pH

| Sample | pH   | Reistivity ( $\Omega\text{m}$ ) | Sheet resisrnce $\times 10^8$ ( $\Omega\text{sq}$ ) |
|--------|------|---------------------------------|---|
| 15A    | 9.0  | 64.0                            | 1.4   |
| 15B    | 9.2  | 74.2                            | 1.8   |
| 15C    | 9.6  | 80.0                            | 2.2   |
| 15D    | 10.3 | 104.9                           | 3.2   |

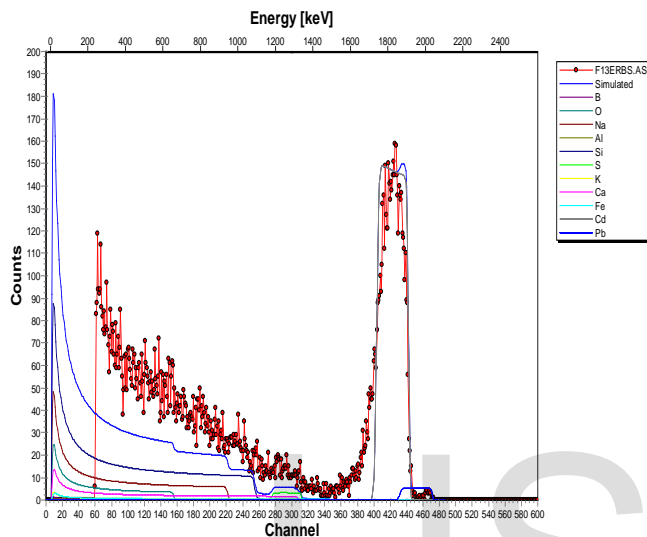


Fig. 3: RBS micrographs for cadmium lead sulphide thin film annealed at 150 °C. Layer 1: Thickness: 552 nm, Compo: Cd 54.27 %. Pb 2.19 %. S 43.54 %. Layer 2: Thickness: 677894 nm Compo: Si 31.97 % . O 32.89 %. Na 25.85 %. Ca 1.64 %. Al 0.25 %. K 1.05 %. Fe 0.38 %. B 5.89 %. Layer 1 refers to thin film deposit while layer 2 refers to substrate.

### 3.4 Resistivity Analysis Result

The four point probe test revealed the resistivity of film to be from 6.4  $\Omega\text{m}$  to 104.9  $\Omega\text{m}$  with resistivity increasing with bath pH. A pH increase connoted addition of more  $\text{OH}^-$  in the bath. This decreased the concentration of metal ions present, specifically  $\text{Pb}^{2+}$  and  $\text{Cd}^{2+}$  leading to decrease in the deposition rate and hence decrease in thickness of thin film grown. In TF formation, deposition rate usually rises rapidly after nucleation until the rate of deposition equals that of dissolution to enable thin film attain a terminal thickness [23]. Lower cadmium and lead ions at terminal thickness implies less conducting film and hence higher resistivity. The variation of thin film resistivity,  $\rho$  with chemical bath pH is as shown in figure 4 and table 4 where resistivity is seen to clearly increase with pH. Such trend has been reported elsewhere for polyaniline (PANI) thin film where pH of the solution strongly affected the oxidized state of the PANI thin film and was capable of converting it into reduced state [24].

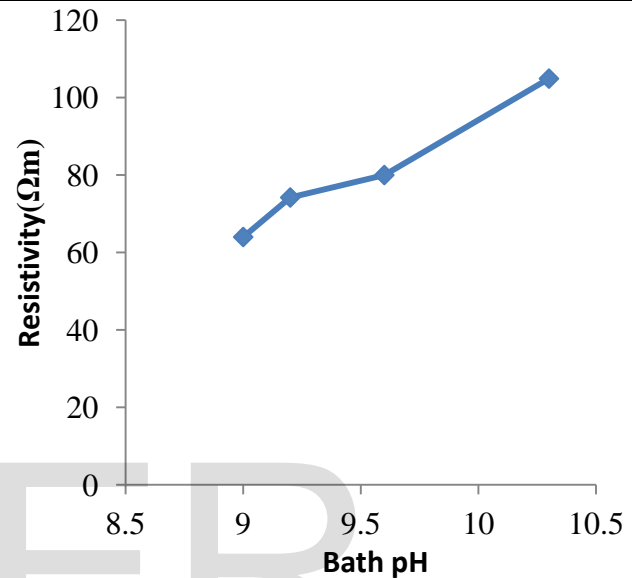


Fig.4: Plot of resistivity of thin film against bath pH

## 4 CONCLUSION

Chemical bath deposition technique, in which the acidity of bath were altered, was used to synthesize improved or doped grades of cadmium sulphide thin films. Resistivity profiles done on the thin film surfaces revealed that the pH variation clearly increased the thin film resistivity; Rutherford backscattering done on the films showed the alteration of bath pH changed the percentage abundance of film elements and improved its surface morphology.

## REFERENCES

- [1] V. Stefko, "Vacuum deposition of stoichiometric thin films of II - VI sulphide semiconductor", *Sov. J. Commun. Techno. Electron*, 36, 1991.
- [2] W. Zhang, J. Hu, Z. Wang, H. Xian and S. Gu. "Microstructure and optical properties of  $\text{As}(\text{S}_x\text{Se}_{1-x})_3$  glasses in VIS-NIR region", *Chalcogenide Letters*, 12(7), 389-397, 2015.
- [3] M. Banerjee, A. Sharma, and L. Chongad, "Effect of doping Pb on the structural and optical properties of nanostructured CdS films", *Research Journal of Recent Sciences*, 2, 322 - 325, 2013.
- [4] P.K. Nair, L. Huang, M.T.S. Nair, H. Hu, E.A. Mayers and R.A. Zingaro, "Optical characterization of chemical bath deposited bismuth copper sulphide thin film", *J. Materials Research*, 12, 651,

- 1977.
- [5] J. Britt and C. Ferekids, "Fabrication and characteristics of high efficiency thin film CdS/CdTe heterojunction solar cells", *Appl. Phys. Lett.*, 62, 2851, 1993.
  - [6] S.C Eugwu, F.I. Ezema and R.U. Osuji, "Effect of deposition time on the band-gap and optical properties of chemical bath deposited CdNiS thin films", *Turkish Journal of Physics*, 29(2), 105 – 114, 2005.
  - [7] D.A.H. Hanaor, G. Triani and C. C.Sorrell, "Morphology and photocatalytic activity of highly oriented mixed phase oxide thin films", *Surface Coatings Tech.*, 205(12), 3658 – 3664, 2011.
  - [8] D. N. Okoli and A.J. Ekpunobi, "Solar car challenges in environmental transportation problems", *Environmental Studies and Research Journal*, 4(2), 7 – 11, 2004.
  - [9] R.S. Mane and C.D. Lokhande, "Chemical deposition method for metal chalcogenide thin films. Materials", *Chemistry and Physics*, 65(1), 21 - 31, 2000.
  - [10] A.I. Onyia, and M.N. Nnabuchi, "Effect of Pb doping on the energy band gap and electrical properties of CdS thin films grown within polymer matrix in chemical bath deposition Techniques" *Chalcogenide Letters*, 11(6), 297 – 302, 2014
  - [11] A.I. Onyia and M.N. Nnabuchi, "Electrical and optical Characteristics of Sb-doped and annealed nanocrystalline SnO<sub>2</sub> thin films deposited in CBD techniques", *J. Ovonic Research*, 11(6), 285 – 291, 2015.
  - [12] C.D. Lokhande, "Chemical deposition of CdS thin film from acidic bath", *Mater. Chem. Phys.*, 26, 405 - 409, 1990.
  - [13] Y. Chen, J. Tseng, S.H. Lin, T.S. Shen, "Effect of grain size on optical and electrical properties of Ni<sub>80</sub>Fe<sub>20</sub> thin films", *Journal of Magnetism and Magnetic Materials*, 360, 87 – 91, 2014.
  - [14] C.D. Gutierrez, E. Rosendo, H. Juarez, G. Garcia Salgado, T. Diaz, M. Rubin Falfan, A.I. Oliva, P. Quintana, D.H. Aguilar, W. Cauich, M. Ortega and Y. Matsumoto, "Hexagonal phase of CdS thin films obtained by oscillating chemical bath", *J. Electrochemical Society*, 155(2), 2008.
  - [15] S.C. Ezugwu, P.U. Asogwa, F.I. Ezema and R.U. Osuji, "Synthesis and characterization of co-doped CdS thin films grown within a polymer matrix by solution growth technique", *Journal of None-Oxide Glasses*, 2(2), 121 – 127, 2010.
  - [16] H.K. Sharma, "Synthesis and characterization of PVA-encapsulated ZnS nanoparticles", *International Journal of Engineering Sciences and Research*, 5(4), 921 – 927, 2016.
  - [17] A.N. Upadhyay, R.S. Tiwari, K. Singh, "Annealing effect on the thermal conductivity and microhardness of carbon nanotube containing Se<sub>80</sub>Te<sub>16</sub>Cu<sub>4</sub> glassy composite", *Materials Research Express* 5(2), 2018.
  - [18] A.I. Onyia, and C.E. Okeke, "Fabrication and characterization of tin oxide thin films using simple glass spray systems", *J. Physics D.*, *Applied Physics*, 2, 49 – 51, 1989.
  - [19] A.B.C. Ekwealor, "Variations of optical and structural properties with temperature of CrxOy thin films synthesized in a polymer matrix by chemical deposition technique", *Digest Journal of Nanomaterials and Biostructures*, 9(1), 423-433, 2014.
  - [20] B.D. Cullity, "Elements of X-ray Diffraction", New York, NY: Addison Wesley, 40, 1978.
  - [21] T.K. Pathak, V. Kumar, H.C. Swart and L.P. Purohit, "Effect of doping concentration on the conductivity and optical properties of p-type ZnO thin films", *Physica B: Condensed matter*, 480(1), 31 – 35, 2016.
  - [22] G.D. Soraru, G.K.R. Camprostrini, A. Ponzoni, M. Donarelli, A. Kumar and G. Mariott, "The effect of B-doping on the electrical conductivity of polymer-derived Si(B)OC Ceramics", *Journal of American Ceramic Society*, 100(10), 4611 – 4621, 2017.
  - [23] A.J. Ekpunobi and C.E. Okeke, "Electrical resistivity study of galena – an earth's crust Substance", *Environmental Research Journal*, 1(1), 21-25, 2001.
  - [24] R. Ruhel, A. Patil Aviraj, R.S. Jatrakar and Y. Devan Yuan, "Effect of pH on the structural, optical and nanomechanical properties of polyaniline thin films", *Applied Surface Science*, 327(1), 201 – 204, 2016.